Monte Carlo analysis of germanium detector performance in slow positron beam experiments

J. Heikinheimo, R. Tuominen and F. Tuomisto

Aalto University, P.O. Box 14100, FI-00076 AALTO, Finland

E-mail: janne.heikinheimo@aalto.fi

Abstract. Positron annihilation Doppler broadening spectroscopy is one of the most popular positron annihilation vacancy characterization techniques in experimental materials research. The measurements are often carried out with a slow positron beam setup, which enables depth profiling of the samples. The key measurement devices of Doppler broadening spectroscopy setups are high-purity germanium detectors. Since Doppler broadening spectroscopy is one of the standard techniques in defect characterization, there is a demand to evaluate different kinds of factors that might have an effect on the results. Here we report the results of Monte Carlo simulations of detector response in different geometries and compare the data to experiments.

1. Introduction

The Monte Carlo N-particle transport code (MCNP) is one of the most used programs to simulate germanium detector properties [1, 2]. Monte Carlo simulations are a good way to identify and model small details in the detector response that are otherwise difficult or impossible to detect in experimental setups. Monte Carlo simulations have been used earlier, too, to model interactions of annihilation radiation in Doppler broadening spectroscopy. This was done for two HPGe detectors in coincidence, and the goal was to recognize pile-up effects in the measurement setup [3].

The peak efficiency of the germanium detector for the annihilation line is one of the important detector parameters in Doppler broadening measurements. The optimal dimensions for the Ge crystal are different for 511 keV gamma photons than for example for 1332.5 keV photons emitted by Co-60, which is commonly used for determining the detector efficiency. The optimal dimensions for efficiencies of germanium detectors with a specific volume were obtained by simulating coaxial detectors with different diameters and thicknesses with typical annihilation-detector geometry. The effect of the thickness of a steel plate placed between the photon source and the detector was analyzed by comparing measurements with different steel thicknesses to the corresponding simulations with the 511 keV gamma line alone.

To simulate the final spectrum of the Doppler broadening radiation, ab initio theoretical predictions of the electron-positron momentum distribution were used as source distribution. Here, GaN bulk and Ga vacancies in GaN were used for analyzing how different factors in the measurement setup affect the final results [4, 5].

2. Methods

2.1. Model for MCNP simulations

Generally, measured and simulated results correspond well to each other for high purity germanium detectors. The difference in detector efficiency could still be of the order of 10 %. Monte Carlo methods tend to overestimate the detector efficiency in the model based on the information from the suppliers [6, 7]. The difference could be caused by thicker dead layer or transition zone in germanium crystal, which changes the dimensions of the active region. The correspondence between the simulated and experimental results has been found by carefully adjusting the dead layer and crystal dimensions [8, 9, 10].

In this work, the dimensions for the germanium detector, crystal, and dead layers are obtained from the technical data provided by manufacturer (Canberra Industries, Inc.). The dimensions for the detector that has been used also in the Monte Carlo model are described in figure 1.

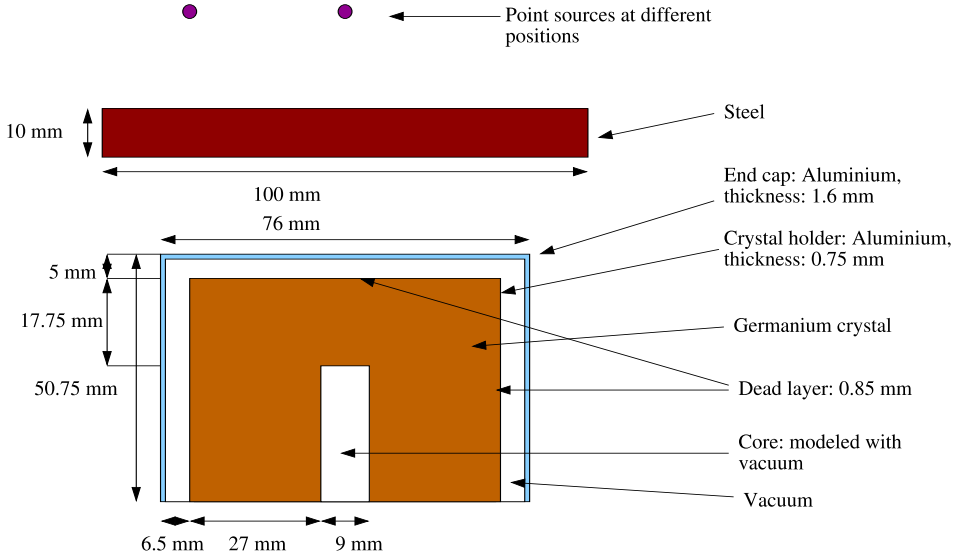

Figure 1. A scheme of the model used in the Monte Carlo simulations. Germanium detector dimensions have been chosen according to the detector that was used in the experiments.

2.2. Photon interactions in MCNP program

The physical treatment for photons includes the photoelectric effect, pair production, incoherent (Compton) scattering, coherent (Thompson) scattering, and fluorescent photons after photoelectric absorption. The electrons are treated in this work according to a thick-target bremsstrahlung model (TTB), where electrons travel in the direction of the incident photon and are immediately stopped.

In photoelectric effect, a photon gets absorbed completely giving its energy to release one electron in an atom and to the kinetic energy of the electron. Recombination effects in the exited atom are also taken into account. These effects could result as fluorescent photons and/or Auger electron.

In pair production, the energy of the photon goes to the creation of the electron-positron pair and to their kinetic energies. The kinetic energy of the electron-positron pair is

$$E_{\pm} = E_p - 2mc^2, \quad (1)$$

where E_p is the initial photon energy and mc^2 is the rest energy of an electron. In this work, positrons and electrons from the pair production were treated according to TTB. When positron energy is below

electron energy cutoff (defined in MCNP), it is considered to be annihilated with an electron producing two photons going to the opposite directions with an energy of mc^2 = 511 keV.

In Compton scattering, a photon is scattered from a free electron. In this event, the objective is to determine the energy of the scattered photon E' and $\mu = \cos(\theta)$ for the angle θ of deflection from the line of flight. The differential cross section for the process is given by the Klein-Nishina formula

$$K(\alpha,\mu)\mathrm{d}\mu = \pi r_0^2 \left(\frac{\alpha'}{\alpha}\right)^2 \left[\frac{\alpha'}{\alpha} + \frac{\alpha}{\alpha'} + \mu^2 - 1\right]\mathrm{d}\mu, \quad (2)$$

where r_0 is the classical electron radius and α and α' are the incident and final photon energies in units $\alpha = E/mc^2$ and $\alpha' = \alpha/(1 + \alpha(1 - \mu))$. MCNP uses the modified Klein-Nishina formula for incoherent scattering

$$\sigma_I(Z,\alpha,\mu)\mathrm{d}\mu = I(Z,\nu)K(\alpha,\mu)\mathrm{d}\mu, \quad (3)$$

where $I(Z,\nu)$ is an appropriate scattering factor and $\nu = \sin(\theta/2)/\lambda$.

Thomson scattering involves no energy loss, and so is only a photon process which doesn't produce electrons. The differential cross section for Thomson scattering is

$$\sigma_2(Z,\alpha,\mu)\mathrm{d}\mu = C^2(Z,\nu)T(\mu)\mathrm{d}\mu, \quad (4)$$

where $C(Z,\nu)$ is a form factor and $T(\mu) = \pi r_0^2(1 + \mu^2)\mathrm{d}\mu$ is the energy-independent Thomson cross section.

3. Results

3.1. Optimization of the Ge crystal dimensions for detector efficiency

It is not always possible or even necessary to have custom designed detectors for slow positron beam measurements. If the detector resolution, peak-to-Compton ratio, and efficiency are sufficient for Doppler broadening measurements, the detector will suite well for its purpose even though its dimensions are not optimal for 511 keV gamma measurements. However, high-purity germanium is challenging and expensive to manufacture and the volume of the high-purity germanium crystal might show up in the detector price tag. Greater volume also generally increases detector capacitance and deteriorates energy resolution.

The optimization was performed with the source in the central position and 2 cm away from the end cap of the detector. The efficiency optimization was done for three different germanium volumes with a coaxial geometry. The results from the iteration are illustrated in figure 2. For V = 80 cm^3, the optimum was found when diameter was 6.8 cm and thickness 2.2 cm. Correspondingly, for V = 142 cm^3, the diameter was 8.2 cm and thickness 2.7 cm, and for V = 200 cm^3, the diameter was 9.2 cm and thickness 3.0 cm. For differently sized crystals, the optimal dimensions were found when the diameter-to-thickness ratio was around 3.

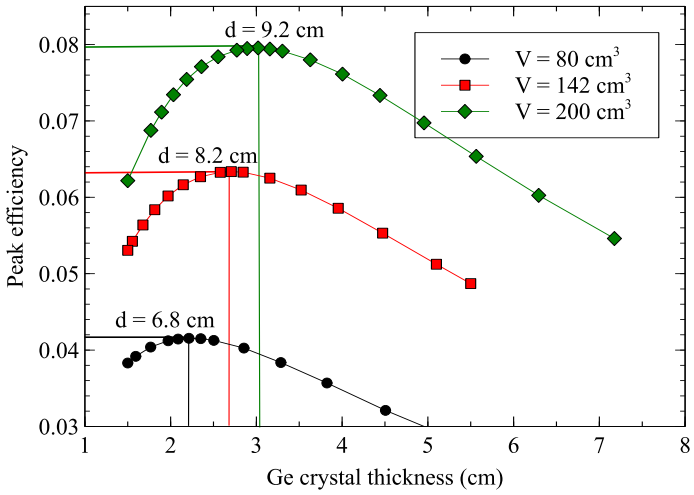

Figure 2. Detector efficiency optimization for three constant volumes.

3.2. Steel thickness and background effects

In positron laboratories, the most common vacuum material is stainless steel (with low magnetic permeability). Here, steel plates with different thickness were placed in between the source and the detector. The source was placed in the experiments and simulations at the central position and 5 cm away from the end cap of the detector

The source in this experiment was Na-22 with thin aluminum wrapping, and its activity was defined with the coincident method to be 78 ± 4 kBq. It was packed to the familiar sandwich package normally used in positron lifetime measurements. The sample material was p-type Si(100).

Figure 3 shows experimentally obtained results for different steel thicknesses. The spectra have been normalized to the same value, or more specifically, the S-regions have been normalized. The spectra behave expectedly in the sense that steel is known to be a rather good shielding material to gamma rays. So, when S-regions are normalized, the background level increases. Especially Compton scattering in steel can potentially increase background in the low-energy side right next to the annihilation peak. It should also be noted that Na-22 daughter nuclide (Ne-22) emits a 1.28 MeV gamma photon. This increases the background in the high-energy region and the effect of steel is visible also there. It is clear that the greater background caused by steel increases the error for *W*-parameter. The effect of steel on the *S*-parameter should be minor.

In the Monte Carlo simulations, the source-detector setup was similar otherwise but the positron annihilation was modeled as a 511 keV point source i.e. without Doppler broadening. The background radiation was not included to the source, either. The results for simulations with different steel thicknesses (modeled with pure iron) are shown in figure 4. When annihilation peaks are normalized to the same value, one can immediately see from the spectra how much the lower energy background next to the annihilation peak is affected by the Compton scattered photons in the steel.

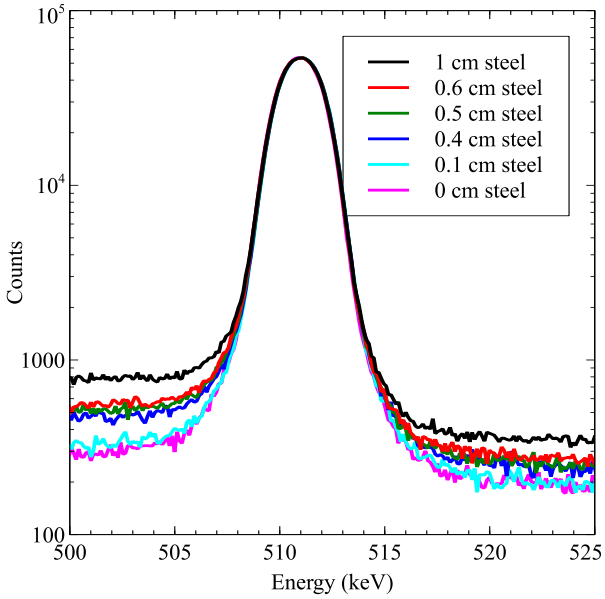

Figure 3. The effect of steel on the annihilation peaks, when the S-parameter region is normalized to the same value.

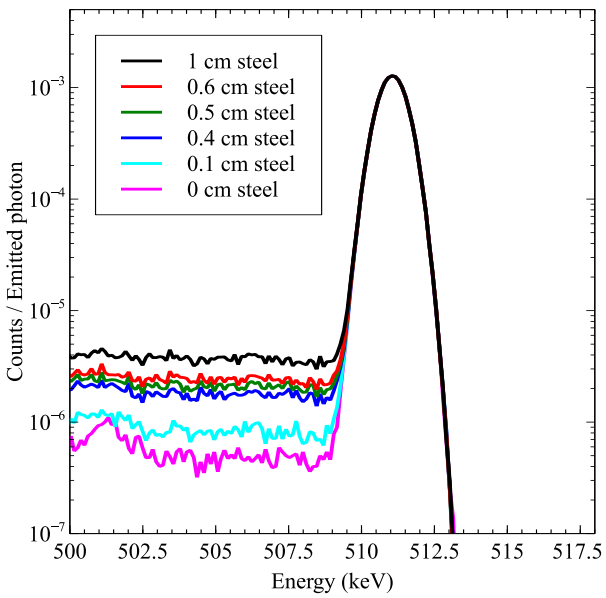

Figure 4. Results of Monte Carlo simulations for the germanium detector, when steel plates of different thicknesses were placed between the source and the detector. The steel plates were modeled in these simulations with pure iron.

3.3. Monte Carlo simulated cases for GaN and Ga vacancy in GaN

In order to get simulated results for Doppler broadening spectrum, results from first principles calculations were applied as a source distribution in the MCNP program. Figure 5 presents a measured ratio curve for the Ga vacancy in GaN [11]. It is followed by results obtained with the first principles calculations and finally the Monte Carlo simulated curve [4]. Here the detector resolution was 1.35 keV at 511 keV. Only the Compton background was taken into account in the background reduction since incomplete charge collection or pile up effects don't exist in the simulations.

As one can see from the figure 5, detector cover or other small details described in figure 1 (without steel) don't have an effect on the gamma interactions so that the ratio curve would change. Changing the source position to 3.15 cm off the axis and keeping the distance from the end cap didn't result in any changes in the ratio curve (the anisotropy of the electron-momentum distribution is not taken into account). Also placing 0.5 cm and 1 cm iron in between the source and the detector didn't result in changes big enough to be clearly separable from the original Monte Carlo simulated spectrum. Iron effect on the ratio curve is presented in figure 6. Changing germanium crystal dimensions didn't show any changes in the ratio curve, either. In all the cases, the *S*- and *W*-parameters remained unchanged.

It is known that the resolution changes the ratio curves. In the Monte Carlo simulations, resolution was applied by sampling the Gaussian distribution. Clear changes in the ratio curves and *S*- and *W*-parameters are obtained when the resolution changes 0.3 keV from the original value. The results are displayed in figure 7.

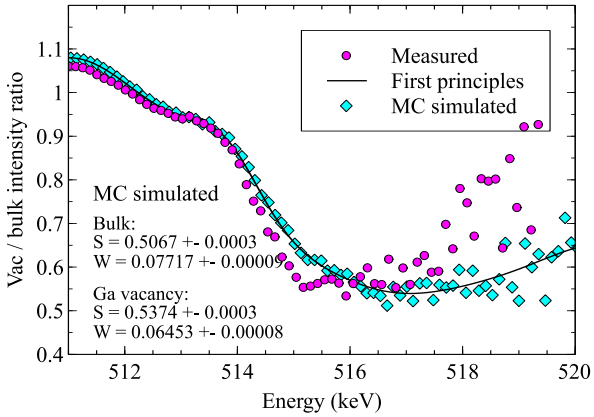

Figure 5. Ratio curves for Ga vacancy in GaN. In the Monte Carlo simulation, the source was placed at the central position 2 cm away from the end cap of the detector. Experimental data is from [11].

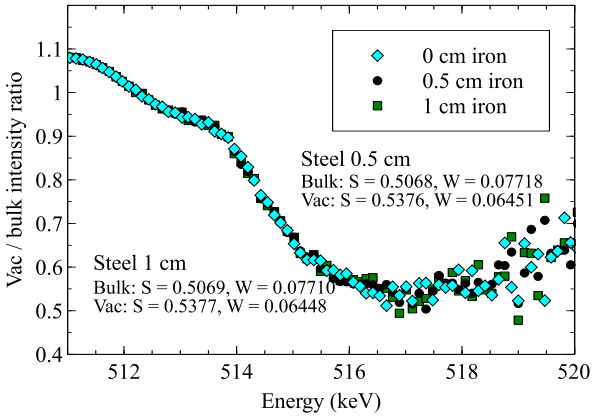

Figure 6. Iron effect on the Ga vacancy in GaN ratio curve. Iron plate is placed in between the source and the detector.

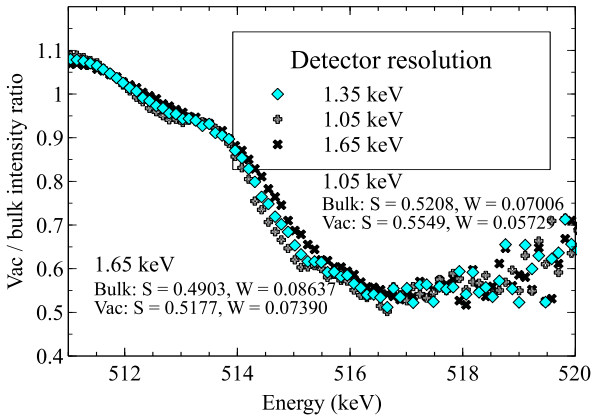

Figure 7. Ratio curves for Ga vacancy in GaN when resolution is varied.

4. Conclusions

With the Monte Carlo simulations, many detector properties could be simulated including final Doppler broadening spectra. However, one should bear in mind that the simulations show only energy deposited in the germanium crystal and not charged particle collection to the electrodes, for example. Here, the detector efficiency was optimized by changing the coaxial detector dimensions. With the three different volumes, the diameter-thickness ratio was close to 3 when the source is placed 2 cm away from the end cap of the detector.

Also background caused by excess steel in between the source and the detector was studied and compared to the corresponding experimental results. With the Monte Carlo simulations, one can conclude how much small angle Compton scattering in the steel increases background level in the low energy side of the annihilation peak.

Comparing the simulated ratio curves for Ga vacancy in GaN, one can study whether the measurement conditions change the final results significantly. In this study, only change in the detector resolution showed clear changes in the ratio curve and in the *S*- and *W*-parameters.

The Monte Carlo results obtained in this work could be applied to normal Doppler broadening measurements and 1-D coincidence measurements.

References

[1] J. F. Briesmeister (Editor) 2000 *MCNP^{TM} - A General Monte Carlo N-Particle Transport Code Version 4C Manual* (Los Alamos: National Laboratory)
[2] R. Berndt and P. Mortreau 2012 *Nucl. Instr. and Meth. in Phys*. A **694** 341
[3] E. do Nascimento, J. M. Fernandez-Varea, V. R. Vanin and N. L. Maidana 2011 *AIP Conference Proceedings* **1351** 216
[4] I. Makkonen and M. Puska 2007 *Phys. Rev.* B **76** 054119
[5] F. Tuomisto and I. Makkonen 2013 *Rev. Mod. Phys.* **85** 1583
[6] J. Rodenas, A. Pascual, I. Zarza, V. Serradell, J. Ortiz and L. Ballesteros 2003 *Nucl. Instr. and Meth. in Phys.* A **496** 390
[7] M.C. Lepy, T. Altzitzoglou, D. Arnold, F. Bronson, R.Capote Noy, M. Decombaz, F. De Corte, R. Edelmaier, E.Herrera Peraza, S. Klemola, M. Korun, M. Kralik, H. Neder, J. Plagnard, S. Pomme, J. de Sanoit, O. Sima, F. Ugletveit, L. Van Velzen and T. Vidmar 2001 *Appl. Radiat. Isot*. **55** 493
[8] J. Boson, G. Ågren, L. Johansson 2008 *Nucl. Instr. and Meth. in Phys.* A **587** 304
[9] C. Agarwal, S. Chaudhury, A. Goswami, M. Gathibandhe, 2011 *J. Radioanal. Nucl. Chem*. **287** 701
[10] N.Q. Huy, D.Q. Binh, V.X. An 2007 *Nucl. Instr. and Meth. in Phys*. A **573** 384
[11] S. Hautakangas, I. Makkonen, V. Ranki, M. J. Puska, K. Saarinen, X. Xu, and D. C. Look 2006 *Phys. Rev.* B **73** 193301